Multiphase Flow Modeling of Molten Material-Vapor-Liquid Mixtures in Thermal Nonequilibrium

Ik-Kyu Park, Goon-Cherl Park
Department of Nuclear Engineering, Seoul National University
Kwang-Hyun Bang*
Division of Mechanical Systems Engineering, Korea Maritime University

This paper presents a numerical model of multiphase flow of the mixtures of molten material-liquid-vapor, particularly in thermal nonequilibrium. It is a two-dimensional, transient, three-fluid model in Eulerian coordinates. The equations are solved numerically using the finite difference method that implicitly couples the rates of phase changes, momentum, and energy exchange to determine the pressure, density, and velocity fields. To examine the model's ability to predict an experimental data, calculations have been performed for tests of pouring hot particles and molten material into a water pool. The predictions show good agreement with the experimental data. It appears, however, that the interfacial heat transfer and breakup of molten material need improved models that can be applied to such high temperature, high pressure, multiphase flow conditions.

Key Words : Multiphase Flow, Vapor Explosion, Phase Change, FCI

Nomenclature

g : Gravity
h : Heat transfer coefficient or enthalpy
h_{fg} : Latent heat of vaporization
I : Internal energy
L : Length scale
p : Pressure
Pr : Prandtl number
$\vec{u}$: Velocity vector
t : Time
T : Temperature

Greek

α : Volume fraction
ε_v : Void fraction
μ : Viscosity
ρ : Density
σ : Surface tension

subscripts

f : Melt
g : Vapor
l : Liquid
s : Saturation

* Corresponding Author,
E-mail : khbang@hanara.kmaritime.ac.kr
TEL : +82-51-410-4365 ; **FAX** : +82-51-405-4790
Division of Mechanical Systems Engineering, Korea Maritime University, 1 Dongsam-dong, Yeongdo-ku, Pusan, 606-791, Korea. (Manuscript **Received** August 23, 1999; **Revised** January 31, 2000)

1. Introduction

Thermal and fluid flow interactions in multiphase flows containing molten materials (or hot particles) and vaporizing coolant (or volatile process liquid) are often interesting in the areas of safety studies involving explosive reactions between hot molten material and coolant-called vapor explosions-as well as the process design of systems operating with multiphase flows with phase change.

Explosive interactions of such multiphase mixture have been often identified as a cause of accidents involving explosions in metal foundries, liquified natural gas transportation, and hydrovolcanism. In particular, nuclear power industry is concerned with the potential risk of

vapor explosions in a hypothetical core meltdown accident. If complete and prolonged failure of normal and emergency coolant flow occurs, decay heat can cause melting of reactor fuel and the molten fuel mass (~3,000 K) may eventually contact with residual coolant water. The molten fuel mass may intermix with coolant water and can be either benignly quenched or resulted in violent explosions, causing damage to plant structures.

Another example that involves thermally interacting multiphase mixture is a pyrolytic waste treatment using molten metals (Corradini et al., 1995). By application of catalytic feature of molten metals, liquid waste is mainly injected into a bath of molten metal and useful elements can be recycled. Such type of waste disposal can treat the high-level waste such as PCB and completely reduce dioxin production safely. However, this technology has not been fully commercialized due to the problem of handling high temperature molten metals.

In a multiphase system containing high temperature molten material, the melt may breaks up into smaller droplets and interacts thermally and mechanically with surrounding liquid and vapor. An illustrative picture of such multiphase mixture is shown in Fig. 1. This picture was obtained in the Japanese experiment in which 20 kg of molten alumina/iron (thermite) at 2,700 K was poured into a water pool (Sugimoto et al., 1992). The melt breaks up as it penetrates into water and forms a multiphase mixture of melt, liquid and vapor.

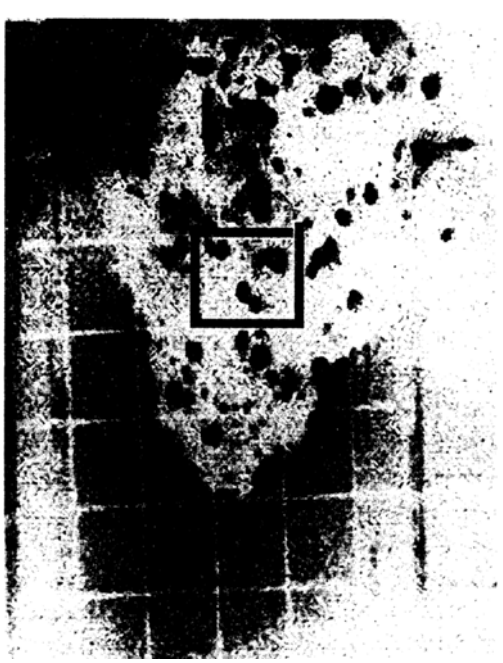

Fig. 1 Illustration of thermal-fluid interaction of molten material-vapor-liquid mixture (Sugimoto, 1992)

In this paper, a numerical model of simulating the multiphase mixture is proposed. Also, to examine the model's ability to predict the experimental data, calculations have been performed for available experiments of pouring hot particles and molten material into a water pool.

2. Mathematical Model

The model is basically transient, two-dimensional, three-fluid model in Eulerian coordinates. The nine field equations for three fluid are couped through mass, momentum, and energy exchange. For molten materials, a breakup model is formulated and the area transport equation is solved to provide interfacial areas. The equations are solved numerically using the finite difference method that implicitly couples the rates of phase changes, momentum, and energy exchange to determine the pressure, density, and velocity fields. A computer program has been written and named TRACER-Ⅱ (TRAnsient Computation of Explosive Reactions).

2.1 Conservation equations

The three-fluid field equations are developed from the Ishii's two-fluid model (Ishii, 1975). For three phases; melt(f), liquid(l), and vapor (g), continuity equations are given as

$$\frac{\partial \alpha_f \rho_f}{\partial t} + \nabla \circ (\alpha_f \rho_f \vec{u}_f) = 0 \tag{1}$$

$$\frac{\partial \alpha_l \rho_l}{\partial t} + \nabla \circ (\alpha_l \rho_l \vec{u}_l) = -J \tag{2}$$

$$\frac{\partial \alpha_g \rho_g}{\partial t} + \nabla \circ (\alpha_g \rho_g \vec{u}_g) = J \tag{3}$$

The mass exchange rates, J, is due to evaporation or condensation of liquid and vapor. A

positive J is the evaporation rate and a negative J is the condensation rate.

Momentum conservations for the melt, liquid, and vapor are as follows:

$$\frac{\partial}{\partial t}(\alpha_f\rho_f\vec{u}_f)+\nabla\cdot(\alpha_f\rho_f\vec{u}_f\vec{u}_f)=-\alpha_f\nabla p+K_{gf}(\vec{u}_g-\vec{u}_f)+K_{lf}(\vec{u}_l-\vec{u}_f)+\alpha_f\rho_f\vec{g} \quad (4)$$

$$\frac{\partial}{\partial t}(\alpha_l\rho_l\vec{u}_l)+\nabla\cdot(\alpha_l\rho_l\vec{u}_l\vec{u}_l)=-\alpha_l\nabla p+K_{gl}(\vec{u}_g-\vec{u}_l)-K_{lf}(\vec{u}_l-\vec{u}_f)-J[\delta(J)\vec{u}_l-\delta(-J)\vec{u}_g]+\alpha_l\rho_l\vec{g} \quad (5)$$

$$\frac{\partial}{\partial t}(\alpha_g\rho_g\vec{u}_g)+\nabla\cdot(\alpha_g\rho_g\vec{u}_g\vec{u}_g)=-\alpha_g\nabla p-K_{gl}(\vec{u}_g-\vec{u}_l)-K_{gf}(\vec{u}_g-\vec{u}_f)+J[\delta(J)\vec{u}_l-\delta(-J)\vec{u}_g]+\alpha_g\rho_g\vec{g} \quad (6)$$

Here, K_{ij} are the momentum transfer coefficients between the phase i and j, and δ is the Heaviside step function, which is the unity for a positive value in parenthesis and zero otherwise.

The energy equations are given as

$$\frac{\partial}{\partial t}(\alpha_f\rho_f I_f)+\nabla\cdot(\alpha_f\rho_f I_f\vec{u}_f)=-\dot{Q}_{fg}-\dot{Q}_{fl} \quad (7)$$

$$\frac{\partial}{\partial t}(\alpha_l\rho_l I_l)+\nabla\cdot(\alpha_l\rho_l I_l\vec{u}_l)=-p\left(\frac{\partial\alpha_l}{\partial t}+\nabla\cdot(\alpha_l\vec{u}_l)\right)-h_{ls}J-R_{ls}(T_l-T_s)+\dot{Q}_{fl} \quad (8)$$

$$\frac{\partial}{\partial t}(\alpha_g\rho_g I_g)+\nabla\cdot(\alpha_g\rho_g I_g\vec{u}_g)=-p\left(\frac{\partial\alpha_g}{\partial t}+\nabla\cdot(\alpha_g\vec{u}_g)\right)+h_{gs}J-R_{gs}(T_g-T_s)+\dot{Q}_{fg} \quad (9)$$

where, $\dot{Q}_{fg}$ and $\dot{Q}_{fl}$ are the heat transferred from melt to vapor and liquid. h_{gs} and h_{ls} are the enthalpy of saturated liquid and saturated vapor under the current pressure, respectively. R_{ls} and R_{gs} are the heat transfer coefficients for liquid and vapor at their interfacial surface.

The complete formulation of momentum and heat transfer rates between phases requires the interfacial area information. The surface area of melt droplets is computed using the interfacial area transport equation proposed by Ishii (1975).

$$\frac{\partial\alpha_f\rho_f L_f}{\partial t}+\nabla\circ\alpha_f\rho_f\vec{u}_f L_f=-\Gamma_{bk} \quad (10)$$

Here, Γ_{bk} is the source term associated with the melt breakup rate during the mixing.

2.2 Constitutive relations

The momentum exchange, heat transfer and phase change are clearly dependent on the flow regime. In three-phase mixture, the flow regime could be defined by a criterion of melt volume fraction, α_f, and void fraction, ε_v in the same manner as two-phase flow. Void fraction is defined as the vapor volume fraction to the sum of liquid and vapor volume, i. e. $\alpha_g/(\alpha_g+\alpha_l)$. For $\alpha_f<0.3$, it is assumed that the melt particles are immersed in two-phase flow of liquid and vapor. The two-phase flow of liquid and vapor has its own flow regimes that are defined in terms of void fraction (Wallis, 1981). In bubbly flow ($\varepsilon_v<0.3$) and churn-turbulent flow ($0.3\leq\varepsilon_v\leq0.7$), vapor bubbles with a certain diameter exist in continuous liquid. In droplet flow ($\varepsilon_v>0.7$), dropwise liquid is surrounded by continuous vapor core. For $\alpha_f>=0.3$ it is assumed that the melt particles form a porous media and then the flows of vapor and liquid are considered as permeating the melt porous media.

2.2.1 Melt breakup

The melt breakup rate is formulated based on the boundary layer striping model proposed by Young (1987), as given by

$$F_{bk}=-C_o\alpha_f\sqrt{\rho_c\rho_f}|\vec{u}_c-\vec{u}_f|/L_f \quad (11)$$

An empirically determined value of 0.245 has been recommended for C_o. Since the change of melt droplet diameter is equal to 1/3 of its volume rate, the source term in the area transport equation (Eq. 10) is

$$\Gamma_{bk}=F_{bk}L_f \quad (12)$$

2.2.2 Phase change

The liquid and vapor phase change rate, J, is defined as

$$J=\frac{1}{h_{fg}}[R_{gs}(T_g-T_s)+R_{ls}(T_l-T_s)] \quad (13)$$

where, R_{gs}, R_{ls}, T_g, and T_l are the heat transfer coefficients for vapor and liquid to the interfacial surface and the temperatures of vapor and liquid, respectively. T_s and h_{fg} are the saturation temper-

ature and the latent heat of vaporization under the current pressure.

2.2.3 Interfacial momentum exchange

The interfacial momentum exchange is primarily due to the drag force. For the dispersed melt ($\alpha_f \leq 0.3$), an exchange formula was proposed by Ishii and Zuber (1979) as

$$K_{ij}=\frac{3}{4}\alpha_i\phi_{ij}\rho_j\frac{C_{Dij}}{L_i}|\vec{u}_i-\vec{u}_j| \tag{14}$$

where, subscripts i, j, and C_{Dij} referred to dispersed phase, continuous phase and drag coefficient between phase i and j, respectively. ϕ_{ij} is a factor which modifies area concentration to account for the existence of third phase (Angelini et al., 1995), and defined as

$$\phi_{ij}=\frac{\alpha_j}{(\alpha_j+\alpha_k)} \tag{15}$$

The drag coefficient, C_{Dij}, is defined for churn flow as

$$i=g,\ j=l,\ C_{Dij}=\frac{8}{3}(1-\varepsilon_v)^2 \text{ and}$$
$$L_i=4(g\Delta\rho/\sigma)^{-1/2} \tag{16}$$

and for bubbly and droplet flow,

$$C_{Dij}=\frac{2}{3}L_i\left(\frac{g\Delta\rho}{\sigma}\right)^{1/2}\left(\frac{1+17.67[f(\alpha_i)]^{6/7}}{18.67f(\alpha_i)}\right)^2 \tag{17}$$
$$i=g,\ j=l,\ \varepsilon_v\leq 0.3,\ f(\alpha_i)=(1-\varepsilon_v)^{1.5}$$
where, $i=l,\ j=g,\ \varepsilon_v>0.7,\ f(\alpha_i)=\varepsilon_v^3$
$$i=f,\ j=g,\ l,\ f(\alpha_i)=(1-\alpha_j)^{1.5}$$

For bubbly flow ($\varepsilon_v<0.3$), the added mass effect, given by Wallis (1981), should be adjusted into the momentum transfer between vapor bubble and liquid.

$$K_{add}=\frac{\alpha_g}{3-\alpha_g}\rho_l\frac{1}{|\vec{u}_g-\vec{u}_l|}\left|\frac{\partial}{\partial t}(\vec{u}_g-\vec{u}_l)\right| \tag{18}$$

For $\alpha_f \geq 0.3$, the melt is assumed porous media. The laminar and turbulent permeabilities are given by Sissom (1972).

$$K_{if}=K_{if}^l+K_{if}^t,\ i=g,\ l \tag{19}$$

$$K_{if}^l=\begin{cases}\dfrac{150\alpha_i\alpha_f^2}{(1-\alpha_i)^3}\dfrac{\mu_i}{L_f^2}, & Re_{i'}<1000\\ 0, & Re_{i'}\geq 1000\end{cases} \tag{20}$$

$$K_{if}^t=\begin{cases}\dfrac{1.75\alpha_i\alpha_f^2}{(1-\alpha_i)^3}\dfrac{\rho_{i'}|\vec{u}_i-\vec{u}_f|}{L_f}, & Re_{i'}>10\\ 0, & Re_{i'}\leq 10\end{cases} \tag{21}$$

$$Re_{i'}=\alpha_f\frac{\rho_{i'}L_f|u_i-u_f|}{\mu_i}$$

The length scale for vapor bubbles and liquid droplets (L_g, L_l) are obtained from the critical Weber number relationship (Park, 1998) and the length scale for melt droplets, L_f, is obtained from the area transport equation (Eq. 10).

2.2.4 Interfacial heat transfer

If the void fraction is less than 0.7, the melt droplets are considered in film boiling regime including a radiation heat transfer. The vapor exists in film adjacent to the fuel droplets as well as separate bubbles if ε_v is large enough. For $\varepsilon_v \geq 0.7$, the melt droplets are surrounded by vapor and exchange heat with vapor by convection and with liquid droplets by radiation. The relevant heat transfer modes in film boiling is illustrated in Fig. 2.

For $\varepsilon_v<0.7$, the heat rates from the melt to the vapor and the liquid are given by

$$\dot{Q}_{fl}=n_f h_r \pi L_f^2 \phi_{fl}(T_f-T_l) \tag{22}$$
$$\dot{Q}_{fg}=n_f h_c \pi L_f^2 \phi_{fl}(T_f-T_s) \tag{23}$$

where, n_f, L_f, h_r, and h_c are the number and length scale of melt droplets, radiative heat transfer coefficient, and convective heat transfer coefficient, respectively (Angenlini et al., 1995). These are given by

$$n_f=6\alpha_f/\pi L_f^3 \tag{24}$$

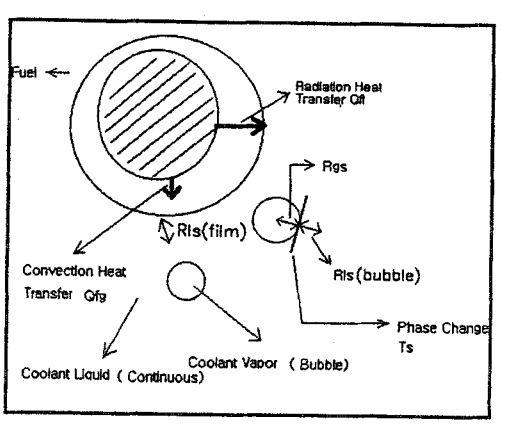

Fig. 2 Heat transfer modes

$$h_r=\sigma_{SB}E_f\frac{T_f^4-T_l^4}{T_f-T_l} \quad (25)$$

$$h_c=2.98\left(\frac{\rho_g k_g[h_{fg}+0.68c_{pg}(T_f-T_l)]}{L_f(T_f-T_l)}|u_f-u_l|\right)^{1/2} \quad (26)$$

The convective heat transfer from the liquid to the interface (Bang, 1994) and also from the vapor film to the interface are given as

$$R_{ls}=n_f\phi_{lf}\pi L_f^2\frac{k_l}{L_f}(2+1.1Re^{1/2}\mathrm{Pr}_l^{1/3}) + n_g\phi_{gl}\pi L_g^2\frac{k_l}{L_g}(2+0.6Re^{1/2}\mathrm{Pr}_l^{1/3}) \quad (27)$$

where, $Re=\frac{\rho_l|\vec{u}_g-\vec{u}_l|L_g}{\mu_l}$

$$R_{gs}=\frac{\dot{Q}_{fg}}{(T_g-T_s)}+2n_g\phi_{gl}\pi L_g^2\frac{k_g}{L_g} \quad (28)$$

For $\varepsilon_v>0.7$, a radiative heat transfer regime is assumed and the liquid exists dropwise in vapor core. The heat from melt is transferred to liquid drops by radiation and to the continuous vapor by convection.

$$\dot{Q}_{fl}=\min(n_l\pi L_l^2,\ n_f\pi L_f^2)\,\sigma E_f E_l(T_f^4-T_l^4) \quad (29)$$

$$\dot{Q}_{fg}=n_f\phi_{fg}\pi L_f^2 h_c(T_f-T_g) \quad (30)$$

Here, σ, E_f, E_l, and h'_c are the Stefan-Boltzmann constant, emissivities of melt and liquid, and the convective heat transfer coefficient from the melt to the continuous vapor, respectively. The h'_c is defined as

$$\alpha_f<0.3\ \ h'_c=\frac{k_g}{L_f}(2+0.6Re_g^{1/2}\mathrm{Pr}_g^{1/3}) \quad (31)$$

where, $Re_g=\frac{\rho_g|\vec{u}_g-\vec{u}_l|L_f}{\mu_g}$

$$\alpha_f\geq 0.3\ \ h'_c=0.91c_{pf}\rho_{g'}|\vec{u}_g-\vec{u}_f|\times Re_g''^{-0.51}\mathrm{Pr}_g^{-2/3},\ Re_g''\leq 50 \quad (32)$$

$$h'_c=0.61c_{pf}\rho_{g'}|\vec{u}_g-\vec{u}_f|\times Re_g''^{-0.41}\mathrm{Pr}_g^{-2/3},\ Re_g''>50$$

where, $Re''_g=\frac{\alpha_g\rho_g|\vec{u}_g-\vec{u}_l|L_f}{6\alpha_f\mu_g}$

In this regime, continuous vapor can be superheated and convective heat transfer occurs from vapor to liquid droplets. Thus, the interfacial heat transfer functions between the continuous vapor and liquid droplets are given by

$$R_{ls}=2n_l\phi_{lg}\pi L_l^2\frac{k_l}{L_l} \quad (33)$$

$$R_{gs}=n_l\phi_{lg}\pi L_l^2\frac{k_g}{L_l}(2+0.6Re^{1/2}\mathrm{Pr}_g^{1/3}) \quad (34)$$

where, $Re=\frac{\rho_g|\vec{u}_g-\vec{u}_l|L_l}{\mu_g}$

The liquid and vapor always move from non-equilibrium state to equilibrium state through phase change. However, the superheated liquid and supersaturated vapor in the subcritical region must be allowed since separate energy equations are solved for liquid and vapor with the phase change relation. For this unique need, a simple relation for this nonequilibrium state of water is formulated using saturation properties and constant specific heat. The NBS/NRC Steam Tables are used for the equilibrium state properties. The detail relations are found in the work by Park (1998).

The nine field equations are coupled through mass, momentum, and energy exchange relations, and solved numerically using the finite difference method to determine pressure, density, and velocity fields. The numerical frames and solution algorithm are built based on the two-phase flow solver, K-FIX program (Rivard and Torrey, 1977).

3. Results and Discussion

To examine the model's ability to predict the experimental data, a set of calculations have been performed for QUEOS (Meyer, 1997) and FARO (Magallon and Hohmann, 1995) experiments. The QUEOS data are very useful for investigating the effectiveness of heat transfer models because heated solid particles are poured into a water pool thus the breakup of melt is not considered in this case. In FARO tests, molten mixture of uranium dioxide and zirconium dioxide at 3,000 K was poured into the water pool of high pressure chamber (50 bars).

3.1 QUEOS-32 calculation

In QUEOS-32 test, 14 kg of 4.95 mm-sized zirconia solid spheres at 1,545℃ was poured into water of 1 m depth at 98.5℃ under atmospheric pressure. This case of solid particles did not need a breakup model, thus it rendered an

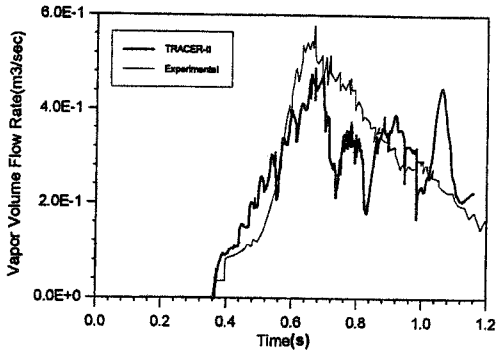

Fig. 3 Predicted vapor flow rate in QUEOS

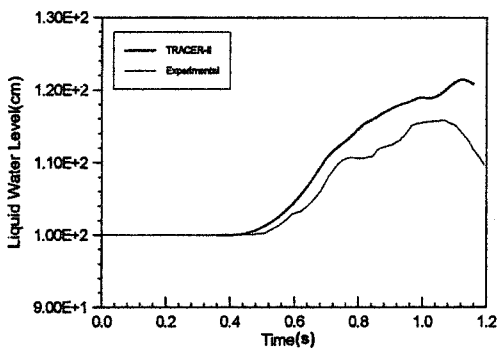

Fig. 4 Predicted liquid water level in QUEOS

evaluation of the heat transfer models. The QUEOS chamber was 70×70 cm rectangular shape, but it was wide enough that the hot spheres did not contact the wall. This allowed a circular geometry for calculations due to its axisymmetric nature. The mesh sizes were 5 cm in radial and 10 cm in axial direction. The initial time step was set to 100 μs. The measured quantities were steam flow rate out of the chamber and liquid water level to compare with the calculation.

The predicted vapor flow rate out of the chamber is shown in Fig. 3. The vapor flow began when the heated particles were delivered onto the liquid (0.4 sec). Then, the flow rate was getting larger until the end of pouring (0.7 sec). The fluctuating behavior of the calculated vapor flow rate seems to be caused by the two-phase flow condition at the chamber exit where the piping system is connected in the actual experiment. In the calculation, the test chamber was treated as a cylindrical pool without a piping model. The gradient-free boundary condition was applied to the exit area. A variation of vapor quality in

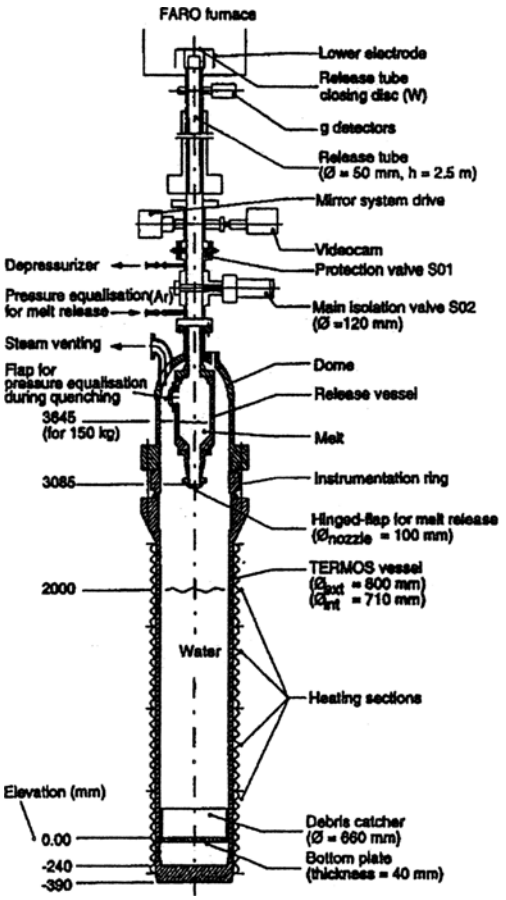

Fig. 5 FARO experimental facility (Magallon, 1995)

exiting flow may cause this fluctuation. It appears, however, that the overall vapor flow seems to agree quantitatively with the data.

The predicted water level swelling is shown in Fig. 4. The level swell also began when the heated particles were delivered into water, and rose until the vapor release rate became larger than the vapor generation rate in the pool. The calculation generally overpredicted the liquid level swell due to to the fact that the liquid-vapor interface can smear in a computational cell and numerically propagate because the current model is built on the Eulerian coordinates. It appears, however, that the prediction of QUEOS test by the present model shows qualitatively and quantitatively reasonable agreement with the data, when considering the complex nature of the physical processes involved.

3.2 FARO-L14 Calculation

In FARO L-14 test, the melt (UO_2+ZrO_2) mass was 125 kg and the initial melt temperature was 2,800℃. A schematic view of the test facility is shown in Fig. 5. The release diameter of melt jet was 0.1 m. The inner diameter of the circular test chamber was 0.71 m. The saturated water at the initial pressure of 5.0 MPa was filled up to 2 m deep in the 3 m high chamber (melt release point to bottom). After the melt was released the chamber pressure rose to 7.8 MPa in 2.4 seconds.

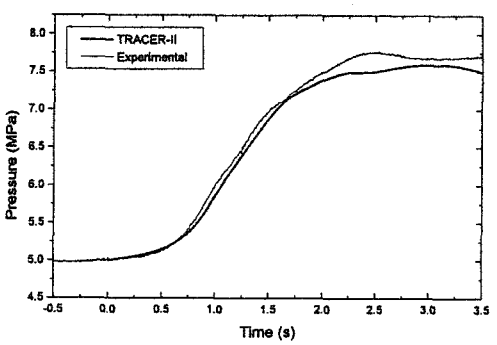

Fig. 6 Predicted chamber pressure in FARO L-14

In calculation, the chamber was treated as axisymmetric. The mesh sizes were 5 cm in radial and 10 cm in axial direction. The initial time step was set to 100 μs. The melt was injected at a constant speed of 2.07 m/s for one second.

The predicted test vessel pressure of FARO L-14 test is shown in Fig. 6 with the experimental data. The present model predicts the data in good agreement. The sizable disagreement after two seconds from the melt pouring seems to be caused by the test facility's unique feature of steam exit flow and associated steam condensation, which is beyond the capability of the present model. In the experiment, the leading edge of the melt fell down 1 m of free space and hit the water surface in 0.45 second. The melt continued to penetrate into the water pool, reaching the chamber bottom in 0.95 second. Such melt flow is illustrated in Fig. 7. In this figure, the predicted melt volume fractions at 0.5 s and 1.0 s are plotted. Due to the Eulerian nature of the model, the melt leading edge

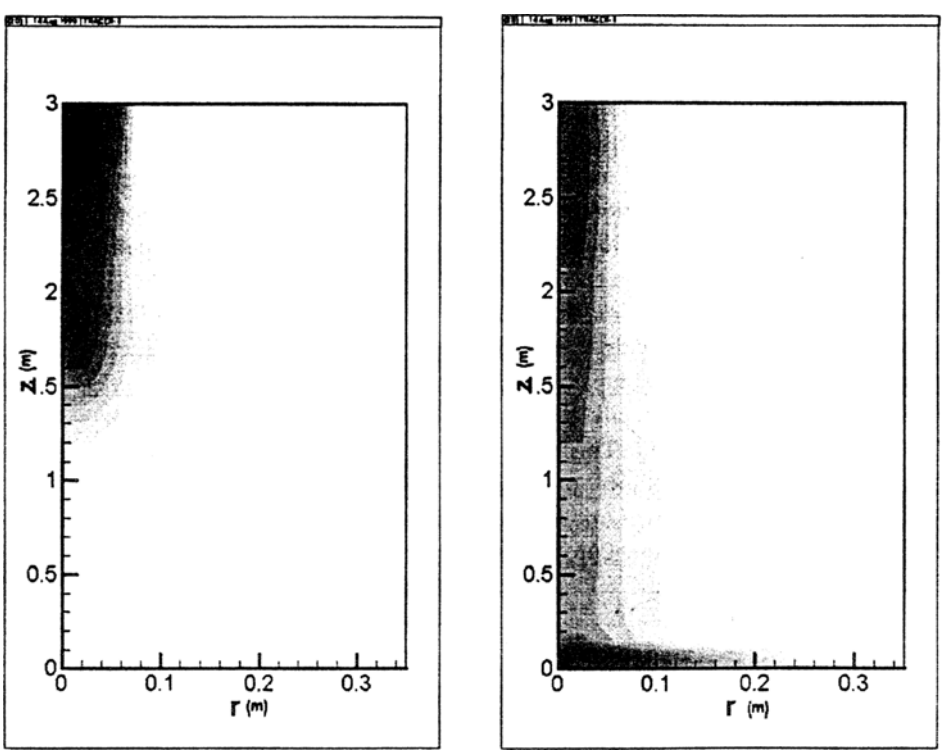

Fig. 7 Predicted melt penetration into water pool (0.5 s and 1.0 s after injection)

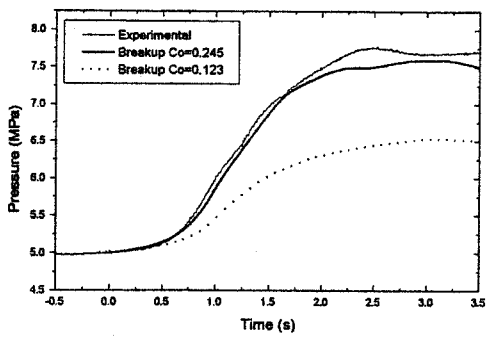

Fig. 8 Effect of melt breakup model Co

advanced faster than the experimental observation.

Despite the complex nature of the problem of hot molten mass pouring into vaporizing liquid, the current formulation of transient, three-fluid multiphase flow model coupled with available relations of interfacial heat and momentum exchanges shows reasonable predictions of the experimental data. However, one fragile feature in the current model may be the melt breakup formulation. The breakup model employed here is based on the data obtained from the single drop breakup in high-speed isothermal flow (Young, 1987), thus it represents only the hydrodynamic feature. In order to investigate the effect of breakup rate in FARO calculation, the constant Co in Eq. (11) was reduced to 0.123, a half of the suggested value of 0.245. The calculation with this reduced breakup rate predicted much lower chamber pressure as shown in Fig. 8. The reduced melt breakup causes less vapor production and the resulting smaller vapor velocity tends to reduce the breakup rate further because the breakup rate is proportional to the relative velocity between the melt and the surrounding fluid. This causes the underprediction of the chamber pressure siginificantly. To build the current model for more general applications, the breakup model should be improved and validated.

4. Conclusion

A computational model has been developed for analyzing thermal and fluid flow interactions in multiphase flows containing molten materials and vaporizing liquid. It is a two-dimensional, transient, three-fluid model in the Eulerian coordinates. The equations are solved numerically using the finite difference method that implicitly couples the rates of phase changes, momentum, and energy exchange to determination of the pressure, density, and velocity fields.

Analyses and comparisons with the experimental data have been performed for the tests of pouring hot particles and molten materials into a water pool. In general, the results show the model's ability to predict the experimental data in reasonable agreement. It appears, however, that the interfacial heat transfer and the breakup of molten material need the improved models that can be applied to such high temperature, high pressure, multiphase flow conditions.

References

Angelini, S., Yuen, W. W., and Theofanous, T. G., 1995, "Premixing-related Behavior of Steam Explosions," *Nucl. Eng. Des.* 155, pp. 115~157.

Bang, K. H., 1994, "Numerical Prediction of Forced Convection Film Boiling Heat Transfer from a Sphere," *Int. J. Heat Mass Transfer*, Vol. 37, No. 16, pp. 2415~2424.

Corradini, M. L. et al., 1995, "INJECT: A Multipurpose Computer Program for Analysis of Molten Pool-Structural Interactions and Associated Recycling Technologies," *U. of Wisconsin-Madison Report.*

Ishii, M., 1975, *Thermo-fluidic Dynamic Theory of Two-Phase Flow*, Eyrolles, Paris.

Ishii, M. and Zuber, N., 1979, "Drag Coefficient and Relative Velocity in Bubbly, Droplet or Particulate Flows," *AIChE J.* Vol. 5, p. 843.

Magallon, D. and Hohmann, H., 1995, "Experimental Investigation of 150 kg-Scale Corium Melt Jet Quenching in Water," *Proc. of 7th Int. Mtg on Nuclear Thermal-Hydraulics, NUREG/CP-0142.* Vol. 3, pp. 1688~1711.

Meyer, L., 1997, "QUEOS, An Experimental Investigation of Premixing Phase with Hot Spheres," *Proc. CSNI Specialist Meeting on Fuel Coolant Interactions*, JAERI-Tokai, Japan, May.

Park, I. K., 1998, *A Computational Model for*

the Mixing and Propagation of Vapor Explosions, Ph. D Thesis, Seoul National University.

Rivard, W. C. and Torrey, M. D., 1977, "K-FIX: A Computer Program for Transient, Two-Dimensional, Two-Fluid Flow," *LA-NUREG-6623*.

Sissom, L. E. and Pitts, D. R., 1972, *Elements of Transport Phenomena*, McGraw-Hill.

Sugimoto, J. et al., 1992, "Fuel-Coolant Interaction Experiments in ALPHA Program," *Proc. 5th Int. Topical Mtg. on Reactor Thermal Hydraulics*, Salt Lake City, Utah, pp. 890~897., Sept.

Young, M. F., 1987, "IFCI: An Integrated Code for Calculation of all Phases of Fuel-Coolant Interaction," *NUREG/CR-5084*, Sandia National Laboratories.

Wallis, G. F., 1981, *One-Dimensional Two Phase Flow*, McGraw-Hill.